Journal of Archaeological Science: Reports 50 (2023) 104067

Contents lists available at ScienceDirect

Journal of Archaeological Science: Reports

journal homepage: www.elsevier.com/locate/jasrep

Insights into the secondary glass production in Roman Aquileia: A preliminary study

Roberta Zanini [a,b], Giulia Moro [a], Emilio Francesco Orsega [a], Serena Panighello [a], Vid S. Šelih [c], Radojko Jaćimović [d], Johannes T. van Elteren [c], Luciana Mandruzzato [e], Ligia Maria Moretto [a,b,*], Arianna Traviglia [b]

[a] Department of Molecular Sciences and Nanosystems, Ca' Foscari University of Venice, Via Torino, 155, 30172 Venice-Mestre, Italy
[b] Centre for Cultural Heritage Technology, Italian Institute of Technology, Via Torino, 155, 30172 Venice-Mestre, Italy
[c] Department of Analytical Chemistry, National Institute of Chemistry, Hajdrihova 19, 1000 Ljubljana, Slovenia
[d] Department of Environmental Sciences, Jožef Stefan Institute (JSI), Jamova 39, 1000 Ljubljana, Slovenia
[e] Arxe s.n.c, Trieste, Italy

ARTICLE INFO

Keywords:
Roman glass
Aquileia
Secondary furnaces
Glass recycling
LA-ICP-MS
INAA

ABSTRACT

A set of 29 glass shards, selected from numerous ones recovered in 2017 in Aquileia (NE Italy), was studied to provide evidence of local glass production for that specific area in antiquity. These shards can be dated between the 1st and the 4th century AD. The chemical composition of glass samples was obtained using laser ablation-inductively coupled plasma-mass spectrometry (LA-ICP-MS) that enables to quantify the concentration of major, minor, and trace elements needed to investigate provenance and compositional groups and sometimes to suggest a chronological frame of the samples. To ensure that the samples are homogeneous enough to perform accurate quantification, some of them were also analysed by instrumental neutron activation analysis (INAA). Most of the chunks, working wastes, and artefact shards considered in this work exhibited similarities among them in terms of composition, which likely indicates that glass working activities were practised at the site of recovery. The analyses demonstrated the presence of both recycled glass and primary glass. Interestingly, the compositional data of raw primary glass point to both Syro-Palestinian and Egyptian regions as sourcing areas, confirming the role of the Roman city of Aquileia as a network node for the trade of goods. In addition, some particularly coloured glass fragments showed a composition typical of glass produced starting from the 1st or 2nd century AD, requiring specific types of furnaces and procedures for its manufacture, and suggesting the possibility of local highly-specialised production. The preliminary results of this work strengthen the hypothesis that Aquileia was a thriving centre, either for working primary glass or for glass recycling and production of objects with particular colours.

1. Introduction

Compared to a number of documented Roman glass workshops, mainly located in Central-Western Europe (Shepherd, 2009; Stern, 2002; Amrein et al., 2012; Da Cruz and Sànchez de Prado, 2015), archaeological evidence of glass working during the Roman period in other European areas like, for example, Italy – (Lepri and Saguì, 2018) - is relatively sporadic and often hard to detect, especially during archaeological surface surveying (Foster and Jackson, 2010). Potential surviving sites require therefore special care to identify, recover, conserve, and interpret glass working evidence. This consideration underlies the work here presented, which focuses on the analysis and interpretation of a selection of specimens from a large glass assemblage identified in 2017 on the plough soil surface during an archaeological field-walking survey in the suburbs of Roman Aquileia (Northern Italy) (Traviglia et al., 2021). The abundant dispersal of archaeological items included working waste (small glass threads, trails, and droplets) and chunks of glass (*i.e.*, blobs of raw or recycled glass – collected, ground-up and re-fused – to be

* Corresponding author at: Department of Molecular Sciences and Nanosystems, Ca' Foscari University of Venice, Italy.
E-mail addresses: roberta.zanini@unive.it (R. Zanini), giulia.moro@unive.it (G. Moro), ors-ef@unive.it (E.F. Orsega), vid.selih@ki.si (V.S. Šelih), radojko.jacimovic@ijs.si (R. Jaćimović), elteren@ki.si (J.T. van Elteren), mandrulu@inwind.it (L. Mandruzzato), moretto@unive.it (L.M. Moretto), Arianna.traviglia@iit.it (A. Traviglia).

https://doi.org/10.1016/j.jasrep.2023.104067
Received 20 October 2022; Received in revised form 24 April 2023; Accepted 2 June 2023

re-melted and eventually worked into proper objects), some of which with embedded refractory materials, found in association with glass shards from a variety of vessels. These items, when found together as part of an 'archaeological assemblage', often indicate the presence of past glassworks (Foy and Nenna, 2001; Lepri and Saguì, 2018). Thus, the overall aim of this work was to analyse the recovered assemblage to establish if it could be linked to the existence of a still buried glass furnace at the location of discovery, and to determine the nature of the activities ongoing at the site and of the products of such a furnace.

Archaeological evidences indicate that during the Roman era, chunks and lumps of raw glass were produced in 'primary' furnaces located near the sources of the principal raw materials (sand and flux), mainly in ancient Palestine and Egypt. These were transported to 'secondary' workshops across the Mediterranean for manufacturing vessels and other glass artefacts (Sayre, 1964; Velde, 1990; Price, 2005; Foster and Jackson, 2009; Jackson and Paynter, 2016). A secondary furnace could use raw glass from a single primary source or receive raw glass made in different primary centres. In the latter case, final objects may exhibit several compositional features (Freestone et al., 2000; Rehren and Freestone, 2015). Additionally, the furnace could produce glass items using recycled glass, which was a common practice in antiquity (Silvestri, 2008). Glass cullet was widely used in the production of new artefacts or traded as recyclable production material to supply other workshops during the first centuries of the Roman Empire.

Aquileia played a significant role in the consumption, trade, disposal, and possible production of glass artefacts during antiquity (Calvi and Tornati, 1968). This is reflected in the large variety of archaeological glass items, including whole vessels or fragments, that have been recovered there over the past two centuries of archaeological research. In addition, ancient inscriptions and written sources have described local glass production (Calvi, 1980). The town's primary involvement in trading recycled material has been conjectured after the recovery of a wood barrel containing 11,000 glass fragments found in the wreck of a Roman ship (the 'Julia Felix') not far from the coast of Aquileia (Buora, 2004; Silvestri, 2008; Silvestri et al., 2008). Despite the numerous clues, no glass melting, recycling, or glassblowing workshops (*i.e.*, secondary furnaces) have been conclusively identified there. Only glass waste recoveries (Buora et al., 2009), a deposit of glass waste intended for refusion in the nearby village of Sevegliano (Buora, 2004), and a disputed identification of the remains of a furnace using geophysics prospection (Groh, 2011) have been reported so far. Therefore, the identification of a glass workshop site in Aquileia is pivotal to clarify whether the city's role in the broader Mediterranean-level glass trade network was merely a place of exchange or also a manufacturing glass centre.

The archaeological assemblage identified in 2017 comprises almost 500 items, which is only a portion of the total items present on the plough soil surface at the time of discovery. The finds were scattered on the topsoil in a suburban area believed to have been used for workshops (Buora et al., 2009). This was due to the repeated ploughing activity that disturbed the sequence of archaeological deposits, causing materials from different contexts to be brought to the surface. Most of the identifiable glass fragments date back to the 1st century BC, with later forms up to the 4th century AD.

This paper reports on the compositional analysis of a selection of the recovered glass items from the Aquileia site using laser ablation-inductively coupled plasma-mass spectrometry (LA-ICP-MS). LA-ICP-MS is considered the most efficient technique for compositional analysis of glass, as it allows for microinvasive quantitative elemental analysis of major, minor, and trace elements in glass with virtually no visible damage (Gratuze et al. 1993; Gratuze et al., 2001; Van Elteren et al., 2009; Wagner et al., 2012; Gratuze, 2013; Panighello et al., 2015; Schibille et al., 2022; Lankton et al., 2022a,b). This analytical technique provides key information to understand the nature of the site. Bernard Gratuze was the first to show and discuss the applicability of this technique in the field of ancient glass analysis (Gratuze et al., 1993, 2001). In particular, a paper by Gratuze in 2013 provides an extensive and detailed presentation of the LA-ICP-MS technique in the field of archaeometric applications (Gratuze, 2013). Since then, several papers about ancient glass analysis by LA-ICP-MS were produced by him and his colleagues at IRAMAT of Orleans (France) (Boschetti et al., 2022; Lankton et al., 2022a,b; Schibille et al., 2022 are among the lastest ones). Some degree of heterogeneity for some elements has not only been reported for ancient glasses but also for reference glasses such as the Corning Museum of Glass Standards. This heterogeneity is caused by issues such as gas bubbles, pigment clusters, metallic aggregates, opacifying crystals, and defects of fusion, amplified by the microscale sampling characteristics of the laser (Bertini et al., 2012; Di Turo et al., 2021; Wagner et al., 2008). To test the microscale homogeneity of some of our samples we compared LA-ICP-MS data with these of instrumental neutron activation analysis (INAA), a technique that can be classified as yielding bulk, macroanalytical data (Jaćimović et al., 2003).

2. Research aim

The overarching aim of this study was to ascertain if the archaeological assemblage identified in the Aquileian suburb could be interpreted as glassworking evidence at the site, pointing to the existence of furnaces once active in that area, and now lying concealed under the topsoil. Chemical analysis would therefore be used to extrapolate key information in the form of major, minor, and trace elements that could be used as univocal indicators of the existence of buried ancient glass furnaces.

Three main research objectives were defined, specifically: *i*) to find a correlation between glass working waste and (fragments of) artefacts that were part of the same assemblage to establish if the composition of their glass was similar and determine if a relationship exists between raw/recycled material and manufactured items; *ii*) to ascertain if potential glass working at the site was operated using primary glass imports or glass recycling procedures (or both); *iii*) to recognise the provenience of raw sources (sand and flux) for glass making.

3. Materials and methods

3.1. The samples

The visual inspection conducted on the approximately 500 items in the assemblage revealed that they belonged to three main categories of objects (Fig. 1): chunks (C), artefacts (A) and working waste (W). The chunks, which were broken glass slags that formed part of larger blocks or slabs (ingots) of raw glass ready to be melted and crafted into specific objects, were predominantly in blue-green colour, with a few specimens in blue and emerald green. The broken artefacts, including rims, bottoms, handles, and walls, were the most numerous finds in the group and were discovered in various colours such as purple, amber, cobalt blue, and emerald green. The lumps, threads, and trails that were by-products of the glass working process were less represented.

Out of the 500 items in the assemblage, 29 samples were selected for analysis, representing each of the three groups and including a variety of different glass colours. Based on their visual features and the comparison with numerous glass objects and fragments preserved and classified in the City Museum, the samples studied here can be dated between the 1st and 4th century AD. Small pieces measuring 3 to 5 mm were carefully removed from each selected item, embedded in epoxy resin, and polished for analysis.

The data extracted from these samples will serve as a baseline for designing a more extensive chemical characterisation plan for a larger number of items included in the assemblage, which will likely provide statistically significant answers in the future.

Fig. 1. Example of the samples collected and their classification in chunks (C), artefacts (A) and waste (W).

3.2. LA-ICP-MS analysis and microhomogeneity confirmation by INAA

Elemental analysis was performed using a 193 nm ArF* excimer laser ablation system (Teledyne Photon Machines Analyte G2, Teledyne, Omaha, USA) connected to a quadrupole ICP-MS (7900x ICP-MS, Agilent Technologies, Santa Clara, USA) was used for elemental analysis. The system was used in the spot-drilling mode, assuming homogeneous composition of the samples, to measure the bulk elemental oxide composition of the samples. Table 1 provides the operational parameters for the spot drilling procedure used. The Analyte G2 is a laser ablation instrument equipped with a two-volume ablation cell (HelEx II) using helium to transport the ablated material from the ablation cell to the ICP-MS; argon was added as a make-up gas before the torch of the ICP. The mass spectrometer was set up in time-resolved analysis mode, measuring one point per mass and acquiring 55 masses. Measurement of the background gases (He/Ar mixture) served to establish a gas blank signal for all masses. A more detailed description of the LA-ICP-MS protocol used in this work can be found in Panighello (Panighello et al., 2015). A sum normalisation calibration protocol was used for the quantification of elements (as their elemental oxides) in the glass samples (van Elteren et al., 2009). The glass standards selected were the following: NIST SRM 610 and 612 (National Institute of Standards and Technology), SGT 2, 3, 4, 5 (Society of Glass Technology), DLH 6, 7, 8 (P&H Developments Ltd.), and standards from the Corning Museum of Glass (CMG B, C, D) (Vicenzi et al., 2002; Wagner et al., 2012). The CMG standards mimic the glass composition of ancient glass. The accuracy and precision of the LA-ICP-MS technique for the bulk analysis of (ancient) glass were determined by measuring the CMG B, C, and D standards via the sum normalization method. In Fig. S1 it can be seen how our data compare to the reported data for 23 elements, whereas in Fig. S2 statistical errors are reported for the whole suite of elements targeted by LA-ICP-MS.

As LA-ICP-MS analysis is a microanalytical technique, only minute amounts of the sample (ca. 50 μg) are analysed in spot-drilling mode. To ensure that the samples are homogeneous enough to perform accurate quantification, some of the samples were also analysed by instrumental neutron activation analysis (INAA). This technique can measure larger samples (0.2–0.5 g in this case), but for a smaller suite of elements, and not including most of the major elements. INAA was performed by the k0-method by irradiating the larger glass samples in the TRIGA Mark II reactor in Ljubljana for 20 h at a neutron flux of 1.1×10^{12} n cm^{-2} (Jaćimović et al., 2003).

Table 1
LA-ICP-MS operating conditions for the LA spot analysis drilling procedure.

Laser ablation (Cetac Analyte G2)		*ICP-MS (Agilent 7900)*	
Wavelength	193 nm	Rf power	1500 W
Pulse length	<4 ns	Sampling depth	6.5 mm
Spot size	80 μm	Isotopes measured	55 isotopes
Fluence	4.08 J cm^{-2}	Acquisition per isotope time/mass	0.01 – 0.05 s
Repetition rate	20 Hz	Total acquisition time	0.999 s
He flow rate (cup/cell)	0.5/0.3 L min^{-1}	Measurement mode	Time-resolved, TRA(1)
Make-up Ar flow rate	0.8 L min^{-1}	Plasma/auxiliary gas flow rate	15/1 L min^{-1}

4. Results and discussion

4.1. Compositional characterization of the samples

The chemical composition of the 29 glass samples as determined by LA-ICP-MS is presented in Table 2, giving the concentrations of 10 major/minor elements (in wt% of their oxides) and 8 trace elemental oxides (in ppm), and including the visually perceived colour of each sample. The remaining 37 trace and ultratrace elemental oxide concentrations are also listed in Table S1 (Supplementary Materials). In Fig. S3 three samples are selected where the LA-ICP-MS concentrations are plotted vs. the INAA concentrations. No large discrepancies are noted from the log–log plots in the concentration range 10^{-3}-10^{6} ppm; however, the fact that in the linear trace element concentration range of 0–30 ppm no significant differences show up, evidences that the samples are sufficiently homogeneous on the microscale sampling level of the laser. From Fig. S3 it follows that heterogeneity issues are minimal; only for Sn and Sc there seems to be a discrepancy between both techniques, possibly due to the erratic distribution of Sn from bronze scrap additions to the glass batch and Sc_2O_3 levels which are very low (ca. 1.5 ppm). Overall, these results indicate that the LA-ICP-MS technique delivers reliable results for the suite of 55 elements.

Based on the concentration data of major elements presented in Table 2 (Si, Ca, Al, Na, Mg, K, P), it can be concluded that all 29 samples are composed of soda-lime-silica glass with natron as flux (Dungworth, 2009; Foster and Jackson, 2009; Foy et al., 2003; Freestone, 2003; Jackson and Paynter, 2016; Wedepohl and Baumann, 2000; World, 2014). This reflects the typical composition of Roman glass between the 1st century BC and 4th century AD, with silica ranging from 58 to 72 % wt., soda in the range 15 to 22 wt%, and levels of Mg, P and K oxides less than 1.5 wt%. Glass with this composition is the most commonly found type in Aquileia (Gliozzo, 2017; Maltoni et al., 2016; Mirti et al., 2000; Silvestri et al, 2018 and references therein). However, three samples (**C30**, **A18**, and **A52**) have unusually high concentrations of Mg, K, and P oxide for natron glass, and they will be discussed separately in Section 4.3.

Calcium and aluminium oxide concentrations were utilized to obtain preliminary information about the glassmaking process and the origin of raw materials. The levels of Ca and Al oxides in the glass are primarily linked to the minerals present in the sands used to create frit and can be utilized to identify the primary glass groups. This was first proposed by Freestone (Freestone, 2003; 2005), who established different typologies of Roman glass through the CaO vs. Al_2O plots. Fig. 2 displays such a plot for the initial characterisation of the samples, revealing a distinct cluster of samples (C1) with a positive linear correlation between Al_2O_3 and CaO (Fig. 2 inset). This suggests that they were made using sands from the same source or from recycled glass. The samples outside the cluster will henceforth be referred to as outliers. Almost all of the samples' calcium and aluminium oxide concentrations match those of North-

Table 2
Chemical composition of the samples: C = Chunk, A = Artefact, W = Waste (in wt % for the major and minor oxides, in ppm for the trace elements). Colours are based on visual perception.

CHUNKS

Sample	Colour	% wt.										ppm						
		Na_2O	MgO	Al_2O_3	SiO_2	P_2O_5	K_2O	CaO	TiO_2	MnO	Fe_2O_3	CuO	CoO	Sr_2O_3	ZrO_2	SnO_2	Sb_2O_5	BaO	PbO
C03	Blue	17.96	0.90	2.52	66.25	0.30	1.19	8.01	0.09	0.63	1.21	2000	1088	588	61	65	3540	315	896
C10	Yellow green	16.70	0.66	2.04	72.01	0.17	1.01	6.19	0.06	0.41	0.50	800	18	504	47	76	215	298	79
C29	colourless	21.09	0.93	1.90	68.79	0.02	0.42	5.45	0.10	0.02	0.59	20	2	527	60	1	5206	167	28
C30	Emerald green	17.17	1.88	1.99	64.95	0.71	1.82	6.42	0.16	0.74	1.35	19,400	50	588	94	1665	2862	347	2333
C31	Blue green	17.95	0.72	2.63	69.14	0.19	0.82	7.14	0.08	0.41	0.61	900	19	590	68	86	361	303	134
C33	Blue green	18.13	0.71	2.17	69.28	0.21	0.91	7.11	0.07	0.46	0.59	1100	24	544	59	112	474	294	155
C39	Blue green	17.72	0.78	2.42	69.12	0.20	0.83	7.28	0.08	0.48	0.73	1000	18	590	64	143	522	308	291
C45	Blue green	17.87	0.76	2.30	69.31	0.22	0.93	7.26	0.07	0.41	0.55	800	20	568	62	194	335	299	119
C46	Blue green	17.96	0.71	2.28	69.68	0.19	0.81	6.98	0.08	0.40	0.54	1000	18	550	65	99	722	277	171
C55	Blue green	17.45	0.66	2.03	71.18	0.16	0.73	6.52	0.07	0.39	0.52	700	18	510	52	69	493	271	146
C56	Light blue green	17.96	0.58	2.01	71.02	0.15	0.68	6.35	0.06	0.42	0.51	600	19	512	52	55	308	270	115
C58	Light blue green	18.41	0.74	2.20	68.97	0.19	0.97	7.13	0.08	0.43	0.54	900	24	559	62	93	539	283	166

ARTEFACTS

Sample	Colour	% wt.										ppm						
		Na_2O	MgO	Al_2O_3	SiO_2	P_2O_5	K_2O	CaO	TiO_2	MnO	Fe_2O_3	CuO	CoO	Sr_2O_3	ZrO_2	SnO_2	Sb_2O_5	BaO	PbO
A14	Blue	19.49	0.58	2.38	67.38	0.15	0.67	7.21	0.06	0.50	1.07	1700	643	576	44	80	682	413	422
A15	Purple	21.38	0.64	2.14	65.86	0.11	0.83	6.62	0.05	1.75	0.41	80	58	682	42	6	212	362	34
A16	Light blue	18.77	0.60	2.35	68.90	0.17	0.77	7.28	0.06	0.36	0.50	300	14	562	52	42	299	272	126
A18	Black (very dark amber)	20.38	2.26	2.53	63.97	0.67	1.58	5.98	0.23	0.47	1.58	700	38	585	130	92	293	286	398
A19	dark yellow green	18.58	0.86	2.39	68.71	0.05	0.54	4.89	0.35	2.13	1.28	40	13	504	251	1	1	487	12
A20	Amber	20.23	1.06	2.33	65.31	0.08	0.75	9.43	0.06	0.10	0.50	20	3	711	47	3	2	241	20
A26	Blue	15.73	0.57	2.06	70.83	0.14	0.49	6.48	0.05	0.65	0.88	1100	588	534	42	4	17,535	259	261
A32	Blue	17.31	0.53	1.91	70.45	0.17	0.78	6.56	0.04	1.01	0.79	1600	1375	578	38	8	44	302	16
A52	Emerald green	18.20	2.51	2.15	62.11	0.96	2.06	6.73	0.17	0.86	1.49	20,900	59	667	115	2012	1212	326	1384

WASTES

Sample	Colour	% wt.										ppm						
		Na_2O	MgO	Al_2O_3	SiO_2	P_2O_5	K_2O	CaO	TiO_2	MnO	Fe_2O_3	CuO	CoO	Sr_2O_3	ZrO_2	SnO_2	Sb_2O_5	BaO	PbO
W01	Light green	17.42	0.52	2.22	70.40	0.13	0.92	7.36	0.06	0.31	0.42	200	8	530	44	27	242	273	212
W04	Light yellow	17.64	0.43	2.37	70.85	0.09	0.64	7.51	0.05	0.02	0.28	10	1	558	44	1	7	236	9
W06	Blue	18.64	0.51	2.32	68.75	0.11	0.52	7.11	0.05	0.71	0.95	800	441	571	47	10	156	630	33
W07	Blue green	18.07	0.76	2.61	68.09	0.17	1.01	8.01	0.07	0.39	0.57	300	18	594	57	41	223	310	118
W37	Yellow green	16.99	0.56	2.53	69.23	0.12	0.83	8.87	0.05	0.28	0.40	10	4	625	43	1	7	258	10
W47	Blue green	18.64	0.63	2.47	68.30	0.14	0.72	7.65	0.06	0.44	0.55	1400	13	569	51	116	374	335	425
W50	Blue green	19.35	0.80	1.83	69.93	0.20	0.66	5.48	0.11	0.61	0.70	400	14	485	93	65	1006	235	148
W51	Dark brownish green	16.82	0.74	2.44	69.22	0.21	0.78	7.12	0.08	0.41	1.80	800	21	509	68	577	397	268	577

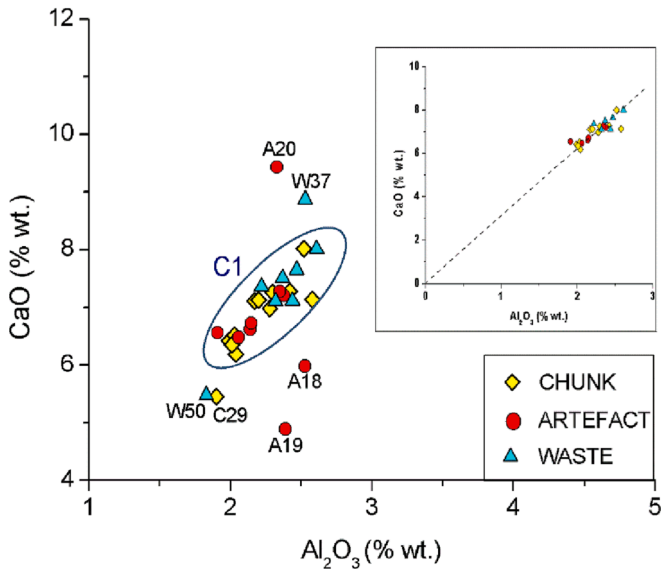

Fig. 2. Plot of CaO vs. Al_2O_3; the oval encloses cluster C1, a compact group of samples with a good linear correlation between calcium and aluminium oxides (shown in the inset).

Western European Roman glass from the 1st to the 3rd century AD (Freestone, 2003). Cluster C1 includes samples with the typical light blue-green hue that characterises vessels produced during the Roman Imperial period.

The purpose of the SrO vs. ZrO_2 plot (Fig. 3) was to determine the source of sands used in primary furnaces as raw materials. In ancient glass, strontium is primarily incorporated as a trace element in lime-bearing materials, such as aragonite or calcite, found in sands. Glass made using coastal sands typically has low ZrO_2 (<100 ppm) and high SrO (>300 ppm) concentrations due to the aragonite in sea shells. On the other hand, glass produced from inland sands, which contains calcium carbonate derived from limestone, shows low SrO (<200 ppm) and high ZrO_2 (>150 ppm) concentrations (Degryse and Freestone, 2010; Freestone et al., 2003; World, 2014). Fig. 3 shows a distinct cluster (C2), which is different from cluster C1 in Fig. 2 due to inclusion of additional samples **A15**, **A52** and **C30** outside of it, while outlier **C29** of C1 falls into C2. Cluster C2 is characterised by high SrO and low ZrO2 contents, indicating the use of coastal sand as raw material for these samples. The similar contents of Sr and Zr oxide contents of C2 samples suggest a

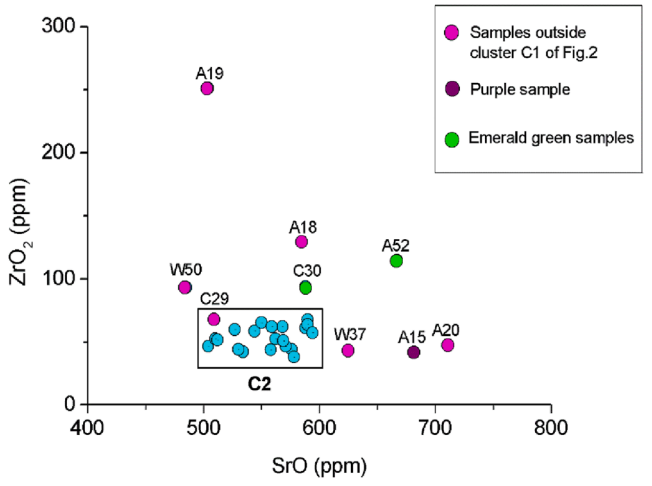

Fig. 3. Plot of ZrO_2 vs. SrO; the rectangle encloses cluster C2 as described in the text. The purple colour of sample **A15** sample is due to the high content of the Mn^{3+} ion.

common origin of the sand or the recycling of glass. Sample **A15** (Fig. 3) has a high level of SrO (682 ppm), which is likely due to the additional content of manganese-strontium bearing minerals, such as rhodochrosite ($MnCO_3$) and pyrolusite (MnO_2), added to obtain the purple colour. Roman natron glasses decoloured by Mn are typically rich in strontium (Jackson, 2005).

The outlined cluster pattern after principal component analysis (PCA) on a set of 31 oxides (Li, Be, B, Al, Si, Ca, Sc, Ti, Cr, Ga, Sr, Y, Zr, Mo, Ba, Th, U) and 14 REE (from La to Lu, except Pm) for all the glass samples is shown in Fig. 4. These oxides have been chosen as those belonging to sands, and excluding all elements that could have originated from minerals added as colorants or opacifiers during the glass-making phase. This multivariate analysis evidences a cluster (C3) whose 21 samples belong also to cluster C1 of Fig. 2, as well as to cluster C2 of Fig. 3, except for the above-discussed sample **A15,** which appears as an outlier due to the presence of manganese minerals.

A similar statistical distribution (Fig. 4, inset) was obtained using factor analysis performed on oxides of Ti, Sr, Zr, Ba, and Cr, the five elements considered by Brems and Degryse (Brems and Degryse, 2014) as the most relevant indicators of the origin of the silica used as raw material. The outliers of cluster C3 will be discussed below.

In summary, the bivariate and multivariate analyses discussed above result in eight outliers (**A18**, **A19**, **A20**, **A52**, **C29**, **C30**, **W37**, and **W50**). The remaining 21 samples (named cluster C3) present a very similar concentration of the elements associated with the raw materials. In cluster C3 all the types of samples, chunks, artefacts, and waste, are represented, suggesting the possibility of glass recycling activity in Aquileia, as detailed below in Section 4.2. On the other hand, the composition of the outliers indicates their origin from imported primary glass, as discussed in Section 4.3.

The samples identified as outliers (**C29**, **C30**, **A18**, **A19**, **A20**, **A52**, **W37,** and **W50**) exhibit varying levels of Ca and Al oxides compared to the samples in cluster C1 (Fig. 2), except for **C30** and **A52**. Samples **A20** and **W37**, which have amber and brown hues, have the highest levels of CaO (9.43 and 8.87 wt%, respectively), while samples **A19**, **C29**, and **W50** have CaO concentrations < 6 wt%, which are lower than those of the C1 group, probably due to different sand sources, poor in calcite and feldspars. The latter two samples contain Na oxide with concentrations higher than 20 wt% (Table 2). Natron glass manufactured with high-purity sand is characterised by low concentrations of CaO, Al_2O_3, and Fe_2O_3, and high Na_2O concentrations, and is typical for glass from the 1st to the 3rd century AD (Jackson and Paynter, 2016). Compared to the sand source that has been used for the production of the samples belonging to cluster C1, the sand used for making the glass of sample **A19** seems to have a different geographical provenance as it contains an elevated ZrO_2 concentration (almost 200 ppm) (Fig. 3).

Among the samples, only sample **W04** shows concentrations of Al_2O_3, TiO_2, and ZrO_2 (2.37 wt%, 0.05 wt%, and 44 ppm, respectively) comparable to those that characterise Rom Mn, primary glass decolourised with manganese, produced in coastal areas of ancient Palestine from 1st to 3rd century (Jackson, 2005; Silvestri, 2008; Silvestri et al., 2008; Jackson and Paynter, 2016; Gliozzo, 2017). Moreover, the low level of Fe_2O_3 (0.28 wt%), and the very low level of MnO (0.02 wt%) denote this sample as a *low Mn* glass according to the definition by Jackson and Paynter (2016).

Sample **C29** is the only colourless sample and has a high concentration of Sb_2O_5 and a very low concentration of MnO, indicating that it was decolourised by antimony oxide (Rom Sb). This sample has a high TiO_2/Al_2O_3 ratio, which is typical of the production of the primary Rom-Sb glass in Egypt, particularly in the area of Alexandria, close to natron sources, as indicated by the high soda content (Schibille et al., 2017). The low concentrations of ZrO_2 and TiO_2 in **C29** are typical for natural quartz sands with a low amount of heavy minerals, providing further evidence of its Egyptian provenance. The distinctive yellowish colour of the sampled chunk is also typical of antimony-decolourised glass and is quite different from the very light blue of Levantine manganese-

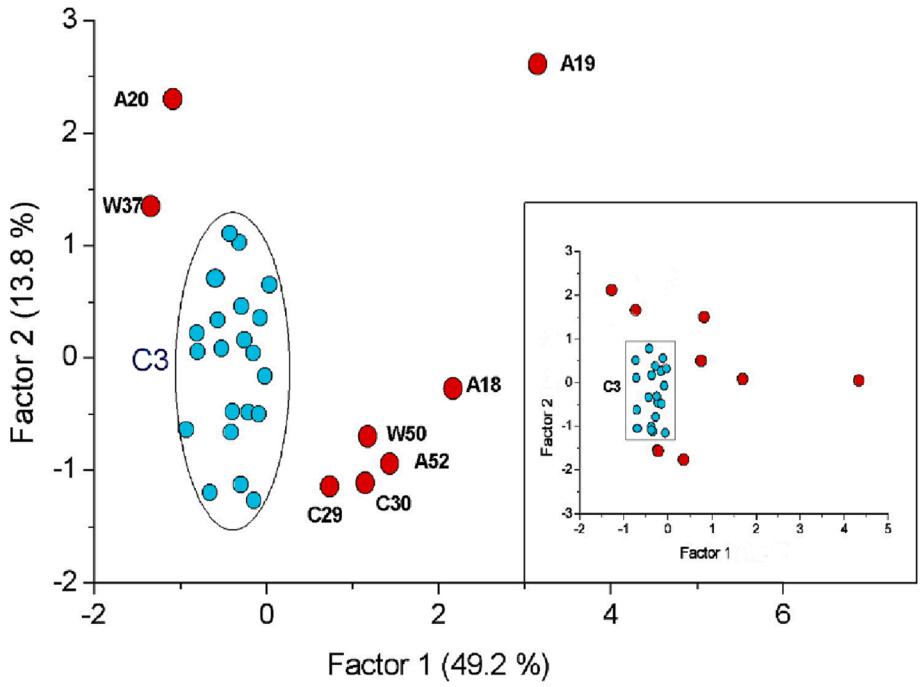

Fig. 4. Factor analysis on the 31 oxides listed in the text (extraction: principal components; rotation: varimax normalised); in the inset the same type of analysis was performed on Ti, Cr, Sr, Zr and Ba oxides.

decolourised glass. The low concentrations of CaO and Al_2O_3 (Fig. 2) suggest that sample **C29** can be dated to around the 1st to 2nd century AD, as antimony glass from the late 2nd and early 3rd century AD normally contains high levels of CaO and Al_2O_3, while in the 4th century, there was a rapid decline in the production of colourless antimony glass (Jackson and Paynter, 2016).

The concentrations of the Al, Ti, and Si oxides in samples **W04** and **C29** are indicative of different geographic areas that supplied the raw materials; if confirmed by additional analysis of a larger sample set of the recovered glass chunks, this would be a first indication that primary glass was sourced by Aquileian glass workshops from both the Syro-Palestinian and Egyptian areas.

The reason to consider the concentration of MnO and Sb_2O_5 in the glass composition is that in Roman glass antimony and manganese were added to the batch for making colourless glass by oxidizing the iron present as an impurity in the raw materials. However, concentrations of MnO and Sb_2O_5 in the glass higher than their natural background level in sand, indicate their intentional addition or accidental addition through cullet recycling. Moreover, the concurrent presence of both these decolourising agents in a glass, as in the C1 cluster, may be an indication of the recycling practice (Section 4.2).

Glass fragment **A19** (blue outlier) shows the typical composition of HIMT1 glass that is characterised by high Fe_2O_3, MnO, and TiO_2 concentrations (Foster and Jackson, 2009). This particular compositional group tends to have low lime (Fig. 2) and high soda contents, in addition to higher concentrations of trace elements, pointing to the use of a less pure silica primary source. Moreover, from a chronological point of view, the latter group is more characteristic of a glass of the early to mid-fourth century as HIMT1 glass was introduced later. Thus, sample **A19** can be dated from the mid-4th century onwards (Foster and Jackson, 2009). It shows high SrO and ZrO_2 concentrations (Fig. 3), similar to HIMT1 glass from Carthage reported by Schibille *et al.* (Schibille et al., 2017), which suggests the use of a sand source located elsewhere than the Levantine coast.

The other five outlier samples seem to have extremely different compositions: *i*) **A20** and **W37** (amber yellow glass), *ii)* **A18** (black glass, actually very dark amber yellow), and *iii)* **C30** and **A52** (emerald green glass). They are discussed in Section 4.2 and are considered key samples to establish the activities of the furnace and the glass manufacturing.

4.2. *Evidence of recycled glass*

The majority of the items sampled in this work show evidence of having been manufactured using recycled glass, as indicated by:

i) The simultaneous presence of the two decolorising agents MnO and Sb_2O_5 in the glass, both at concentrations higher than their natural upper limit values. The presence of both decolorizing agents has never been found in raw glass from a primary furnace (Freestone, 2015). The natural upper limits of Mn and Sb in Roman glass are variable or not always specified in the literature where Roman glass recycling is discussed and some assumed values are determined by the detection limit of the used analytical technique. Sayre (1963) first established an upper threshold of 0.2 % wt for the natural concentrations of both Mn and Sb oxides. Brems and Degryse (2014) report these limits as defined by different authors as follows: 0.1–0.2% (Wedepohl et al., 2011), 0.2% (Sayre, 1963), 0.4% (Brill, 1988), 0.5% (Jackson, 2005) or 1% (Henderson, 1985; Mirti et al., 2000, 2001). Freestone (2005) calculated 250 ppm for MnO and 300 ppm for Sb, that are close to the detection limit of the used technique (EPMA), and later he proposed 200 ppm for MnO in Levantine glass (Freestone, 2015), while Gliozzo (2017) gave a limit of 100 ppm for Sb, and 250 for MnO. Brems and Degryse (2014) on the basis of their studies on the sands conclude that the background upper levels for MnO and Sb are 0.1% wt. and 30 ppm, respectively (80 ppm for Sb2O5). By comparing the different values assumed, it can be stated that samples with MnO concentrations over 300 ppm and Sb_2O_5 over 130 ppm are surely recycled glass known as Rom Mn-Sb glass, obtained through the contribution of Mn and Sb (Rom-Mn and Rom-Sb, respectively).

ii) Levels of heavy metals such as Cu, Co, Sb, Sn, Pb higher than their natural oxide concentrations (lower than 100 ppm) are indicative of recycling (Degryse and Shortland, 2009; Foster and Jackson, 2010; Freestone et al., 2002) if not intentionally added as colouring (Cu, Co), decolouring (Sb) or opacifying (Sb, Sn, Pb) agents. Most of the samples have SnO_2 well above 100 ppm and with a ratio to CuO of the order of

1:10, indicating the introduction of bronze scraps. Lead instead might originate from the Sb minerals (Jackson and Cottam, 2015a,b), in particular through the best known bindheimite and appear in glass from recycling Sb-decolorized glass.

The majority of samples belonging to the Rom Mn-Sb group exihibit the typical Roman green–blue colour that originates from mixing two primary glass types: manganese-decolourised glass (Rom-Mn) and antimony-decolourised glass (Rom-Sb), which are used as part of the recycling process, together with not decolourised glass coloured by iron chromophores Fe^{2+} (light blue) and Fe^{3+} (yellow). The high proportion of MnO compared to Sb_2O_5 in the Rom Sb-Mn samples suggests that glass decolourised with manganese (~90 %) was mostly used for recycling, with antimony (~10 %) being used to a lesser extent. The ratio of the two decolourising agents likely depended on the available glass material. Some sources indicate that Rom-Mn glass was produced in Palestine (Nenna et al., 1997), while Rom-Sb glass was likely made in Egypt (Degryse, 2014; Gliozzo, 2017; Paynter and Jackson, 2019; Barfod *et al.*, 2020). A more extensive analysis of a larger number of samples could provide valuable information for more precise dating.

Only the blue samples, **C03** and **A26**, show comparable amounts of MnO (0.63 and 0.65 wt%, respectively) and Sb_2O_5 (0.354 and 1.75 wt%, respectively), suggesting a production period different from that of the rest of the Rom-Mn-Sb samples. All the blue samples, including **C03**, **A26**, **A14**, **A32,** and **W06**, contain high levels of cobalt oxide, which contributes to the intense blue colouration due to the presence of the powerful blue chromophore Co^{2+} ion.

The samples with an elemental composition that appear to have been made not using recycled primary glass are the eight outliers listed in Section 4.1, in addition to the samples **A32** and **W04**. Specifically, amber **A20**, blue **A32**, yellow-green **W04**, and light yellow **W37**, show amounts of CuO, Sb_2O_5, SnO_2, and PbO below 100 ppm, except for the deep blue sample **A32**, which has a very high cobalt content. In addition, HIMT 1 sample **A19** seems to be a non-recycled glass, as its composition shows high concentrations of iron (responsible for the dark yellow-green colour), manganese, and titanium, typical of this compositional group, but negligible levels of the other heavy metals listed in Table 2.

The recovery of fragments of vessels obtained by recycled glass could be evidence of glass working at the site. The fact that almost all the chunks, artefact fragments, and waste of the preliminary set of glass here analysed are made from recycled glass could be an indication that there were glass working activities at the site and probably an important recycling centre.

4.3. Uncommon glass types

The analysed subset of samples included five fragments that stand out due to their composition, as they are outside the main cluster (C1) in Fig. 2. These fragments have unusual colours such as emerald green (**C30** and **A52**), amber (**A20**), and black (**A18**). Glass with these colours was produced starting from the 1st or 2nd century AD and required specialised manufacturing procedures that were available in a limited number of furnaces (Nikita and Nightingale, 2006; Cagno et al., 2013; Jackson and Cottam, 2015a,b; Traviglia et al., 2021). Therefore, glass with these colours is normally characterised by specific compositions.

The emerald green samples, **C30** and **A52**, contain higher levels of K, Mg, and P oxides (on average 2.2, 1.9, and 0.83 wt%, respectively) compared to Roman natron glass. Such high levels of K, Mg, and P are typically associated with the use of plant ash flux (Arletti et al., 2008), which was not commonly used in the first period of the Roman Empire but gradually replaced natron from the 9th century AD onwards (Gallo et al., 2013). The use of plant ash flux as a reducing agent to achieve the desired emerald green colour in the second step of firing is associated with high levels of K, Mg, and P oxides in glass samples from the Roman period (Jackson and Cottam, 2015a,b). Starting from the middle of the 3rd century AD, plant ash fluxes were used only for producing glass in today's Iraq region (Mirti et al., 2008). However, such glass presents K, Mg, and P oxide contents much higher than in the samples C30 and A52. Emerald green samples **C30** and **A52** have a composition very similar to Roman emerald green glass found in France, England, and Slovenia, starting from the 1st century AD (Jackson and Cottam, 2015a,b). Their composition (Table 2) also indicates the intentional addition of high amounts of CuO (ca. 2 wt%) and Fe_2O_3 (ca. 1.5 wt%), together with significant amounts of Sb_2O_5, PbO, and SnO_2. The elemental Cu/Sn ratios in the **C30** and **A52** samples (10.5 and 11.8, respectively) indicate the addition of copper via bronze scraps. Based on the concentrations of Al_2O_3 and CaO (Fig. 2), the samples **A52** and **C30** could be included in cluster C1, but they can be considered outliers because of their high levels of SrO, ZrO_2 (Fig. 3), and TiO_2 that can be associated to the above-mentioned chromophores and/or opacifiers added to the batch. The combination of the opaque yellow antimonate of lead and tin (or lead antimonate and white tin oxide) with the deep aquamarine blue given by the high copper concentration, results in the typical emerald green colour.

Sample **C30** is one of many emerald green chunks recovered at the site. Given that emerald green glass was used exclusively to manufacture specific forms of glass objects in antiquity (Van Der Linden et al., 2009), the recovery of several emerald green chunks might point to the existence in situ of a secondary furnace specialised in producing them. In this case, the provision of the necessary raw material could have been made either by directly importing raw emerald green glass slags/blocks, or by producing emerald green glass directly in Aquileia using mineral soda glass with the addition to the batch of chromophores, opacifiers, and plant ash. This second hypothesis could be corroborated by the fact that one of the more used plants to obtain ashes for glass production is Salicornia (Henderson, 1985) which grows in saline and swampy environments, like the Lagoon of Grado, few miles south of Aquileia.

Amber sample **A20** has a composition similar to blue-green natron glass, differing from it in low MnO and negligible Sb_2O_5 contents. Amber glass production, and working too, was carried out in specialised centres, using selected raw materials. The amber glass batch was normally coloured during the primary melting phase (Jackson et al., 2018). Similar to other strong colours, amber glass was produced from the early Imperial period to the early 2nd century AD, becoming relatively rare later on (Price and Cottam, 1998). Amber sample **A20** has a high content of CaO (ca. 9 wt%) and SrO (>500 ppm), which suggests the use of coastal sand particularly rich in seashells. The limited level of Fe_2O_3 in the sample (0.5 wt%), due to the presence of natural impurities in the sand source, ensures the right proportion of Fe^{3+} and S^{2-} ions needed to achieve the amber hue (Paynter and Jackson, 2018). To facilitate the development of an amber colour, reducing agents such as charcoal were added to control the redox state of the iron chromophore.

The glassworking sample, **W37**, has a composition typical of primary raw material. The fragment appears to have an opaque, matt surface with a slightly lumpy appearance, as seen in Fig. 1. This is characteristic of trails and dribbles of glass that have fallen into the ash pit of the furnace.

Upon careful observation, sample **A18** appears to have a very dark amber hue that resembles black. In contrast to the previous amber sample (**W37**), **A18** is characterised by high concentrations of CuO, Sb_2O_5, and PbO (ca. 700, 300, and 400 ppm, respectively), which are typically associated with recycling practices in glass batch preparation. Additionally, it exhibits high levels of Fe_2O_3 (1.6 wt%) and TiO_2 (0.33 wt%) and unusually high amounts of K, Mg, and P oxides, like the two emerald green samples (**C30** and **A52**) described earlier. This chemical composition suggests that the glassmakers may have been experimenting with an alternative way to make amber glass by remelting recycled blue-green glass and deliberately adding iron and large quantities of organic reducing agents rich in magnesium to achieve the appropriate conditions for creating amber glass that mimics black obsidian. Black glass was produced from the 1st to the 5th century AD and has been amply studied (Baert et al., 2011; Cagno et al., 2013; Ceglia et al., 2014; Van Der Linden et al., 2009). Only a few known Roman glass vessels

from Northern Europe in the 3rd century AD are considered dark amber/brown, and their colour is due to the iron-sulphur chromophore (Fe^{3+}-S^{2-}–$3O^{2-}$) in combination with the dominant Fe^{2+} ion (light blue) and residual Fe^{3+} ion (pale yellow) achieved under strong reducing conditions (Jackson et al., 2018; Sanderson and Hutchings, 1987; Schreurs and Brill, 1984). A black glass fragment from Adria (Gallo et al., 2013) has a composition similar to sample **A18**, with a comparable content of Fe_2O_3 (1.58 wt%), but its black colour was attributed solely to its high iron content.

5. Conclusions and perspectives

The compositional data reported in this paper were performed to examine an assemblage of glass items resulting from an archaeological survey. The main goal of the study was to determine if the glass items could be indicative of a buried glass furnace at the site of discovery and to identify the type of glass production that took place there. We focused on three objectives to provide sufficient evidence.

The first objective was to determine if there were compositional similarities between the recovered glass-manufacturing waste and the fragments of artefacts found at the site. Elemental analysis of the samples revealed strong similarities in composition, indicating a direct link between the raw materials and the artefacts recovered from the same location. This provided clear evidence of glassworking activities at the site and suggested the potential presence of a glass furnace still partially preserved under the soil.

The second objective was to determine whether the glass found at the site was made from primary raw glass imports or recycled glass, or both. Chemical analyses revealed that mostly recycled glass was used, with occasional use of primary glass. Waste from primary glass, as well as several chunks of recycled glass and artefacts made from both types of glass, were identified, suggesting the potential presence of furnaces that worked with both primary and recycled glass. Additionally, there were indications of specialised production of both black glass vessels (dark amber) and emerald green glass, suggesting the possibility of more than one furnace at the site.

The final objective was to recognise the provenience of the raw sources (sand and flux) for the glass used at the site. The bivariate and multivariate analyses of the sands and flux elements indicate a similar composition for most of the three types of recovered items (C, A, W), which resulted to be recycled glass. Instead, these analyses suggest that some of the raw glass chunks were made of primary glass from both Syro-Palestinian and Egyptian areas. This indicates that the glassworkers in Aquileia were able to source raw glass from both Egyptian and Levantine sources, which is not surprising given that the city of Aquileia was a hub for the trade of goods.

The initial patterns observed in the analytical data of the first subset of samples will provide a foundation for planning future research, which includes analysing the remaining items of the archaeological assemblage found in 2017. Additional studies are currently underway on glass samples recovered from various other sites throughout the suburban regions of Aquileia. We anticipate that these collective results will aid in elucidating the glass manufacturing practices in the area and refining existing theories regarding Aquileia's role as a significant glassworking centre in the Mediterranean area.

CRediT authorship contribution statement

Roberta Zanini: Investigation, Writing – original draft. **Giulia Moro:** Conceptualization, Writing – original draft. **Emilio Francesco Orsega:** Conceptualization, Formal analysis, Writing – review & editing. **Serena Panighello:** Supervision. **Vid S. Šelih:** Investigation. **Radojko Jaćimović:** Investigation. **Johannes T. van Elteren:** Methodology, Writing – review & editing. **Luciana Mandruzzato:** Conceptualization, Supervision. **Ligia Maria Moretto:** Supervision, Writing – review & editing. **Arianna Traviglia:** Conceptualization, Supervision, Writing – review & editing.

Declaration of Competing Interest

The authors declare that they have no known competing financial interests or personal relationships that could have appeared to influence the work reported in this paper.

Data availability

No data was used for the research described in the article.

Acknowledgements

The authors express their gratitude to the *Soprintendenza Archeologia, Belle arti e Paesaggio del Friuli Venezia Giulia* – Superintendency for Archaeology, Fine Arts and Landscape of Friuli Venezia Giulia Region (Dr. S. Bonomi and Dr. P. Ventura) for granting research permissions and for their invaluable support and assistance throughout all phases of the research.

Appendix A. Supplementary data

Supplementary data to this article can be found online at https://doi.org/10.1016/j.jasrep.2023.104067.

References

Amrein, H., Carlevaro, E., Deschler-Erb, E., Deschler-Erb, S., Duvauchelle, A., Pernet, L., 2012. Das römerzeitliche Handwerk in der Schweiz. Bestandsaufnahme und erste Synthesen.

Arletti, R., Vezzalini, G., Biaggio Simona, S., Maselli Scotti, F., 2008. Archaeometrical studies of roman imperial age glass from canton ticino. Archaeometry 50, 606–626. https://doi.org/10.1111/j.1475-4754.2007.00362.x.

Baert, K., Meulebroeck, W., Wouters, H., Cosyns, P., Nys, K., Thienpont, H., Terryn, H., 2011. Using Raman spectroscopy as a tool for the detection of iron in glass. J. Raman Spectrosc. 42, 1789–1795. https://doi.org/10.1002/JRS.2935.

Barfod, G.H., Freestone, I.C., Lesher, C.E., Lichtenberger, A., Raja, R., 2020. 'Alexandrian' glass confirmed by hafnium isotopes. Sci Rep 10, 11322. https://doi.org/10.1038/s41598-020-68089-w.

Bertini, M., Izmer, A., Vanhaecke, F., Krupp, E.M., 2012. Critical evaluation of quantitative methods for the multi-elemental analysis of ancient glasses using laser ablation inductively coupled plasma mass spectrometry. J. Anal. At. Spectrom. 28, 77–91. https://doi.org/10.1039/C2JA30036B.

Boschetti, C., Gratuze, B., Cavalieri, M., Lenzi, S., Schibille, N., 2022. Production or Consumption? Glass Beads from the Roman Villa of Aiano, Tuscany. Europ. J. Archaeol. 25 (2), 196–215.

Brems, D., Degryse, P., 2014. Trace Element Analysis in Provenancing Roman Glass-Making. Archaeometry 56, 116–136. https://doi.org/10.1111/ARCM.12063.

Brill, R.H., 1988. Chapter 9: Scientific Investigations of the Jalame Glass and Related Finds. In: Weinberg, G.D. (Ed.), Excavations at Jalame: Site of a Glass Factory in Late Roman Palestine. University of Missouri Press, Columbia, pp. 257–294.

Buora, M., 2004. Vetri antichi del Museo Archeologico di Udine. I vetri di Aquileia della collezione di Toppo e materiali da altre collezioni e da scavi recenti [WWW Document]. Edizioni Quasar. URL https://edizioniquasar.it/products/1496 (accessed 11.4.22).

Buora, M., Mandruzzato, L., Verità, M., 2009. Vecchie e Nuove Evidenze di officine vetrarie romane ad Aquileia. Quaderni Friulani di Archeologia XIX 51–58.

Cagno, S., Cosyns, P., Van der Linden, V., Schalm, O., Izmer, A., Deconinck, I., Vanhaecke, F., Nowak, A., Wagner, B., Bulska, E., Nys, K., Janssens, K., 2013. Composition data of a large collection of black-appearing Roman glass. Open Journal of Archaeometry 1, 22. https://doi.org/10.4081/arc.2013.e22.

Calvi, M., Tornati, M., 1968. Ricerche tecnologiche. I Vetri Romani Del Museo Di Aquileia. 195–208.

Calvi, M., 1980. Le arti suntuarie, in: Da Aquileia a Venezia. Una Mediazione Tra l'Europa e l'Oriente Dal II Secolo a.C. Al VI Secolo d.C. Milano (Italy), pp. 453–490.

Ceglia, A., Nuyts, G., Cagno, S., Meulebroeck, W., Baert, K., Cosyns, P., Nys, K., Thienpont, H., Janssens, K., Terryn, H., 2014. A XANES study of chromophores: the case of black glass. Anal. Methods 6, 2662–2671. https://doi.org/10.1039/C3AY42029A.

Da Cruz, M., Sànchez de Prado, M.D., 2015. Glass Working Sites in Hispania: What we know. Presented at the Annales du 19e Congrès de l'Association Internationale pour l'Histoire du Verre, Koper, Piran 17-21 septembre 2012, pp. 178–187.

Degryse, P., Freestone, I., 2010. Technology and provenance study of Levantine plant ash glass using Sr-Nd isotope analysis, in: Glass in Byzantium - Production, Usage, Analyses. pp. 83–90.

Degryse, P., Shortland, A.J., 2009. Trace elements in provenancing raw materials for Roman glass production. Geol. Belg. 12, 135–143.
Degryse, P. (Ed.), 2014. Glass making in the Greco-Roman world: results of the ARCHGLASS project, Studies in archaeological sciences. Leuven University Press, Leuven, Belgium.
Di Turo, F., Moro, G., Artesani, A., Albertin, F., Bettuzzi, M., Cristofori, D., Moretto, L.M., Traviglia, A., 2021. Chemical analysis and computed tomography of metallic inclusions in Roman glass to unveil ancient coloring methods. Sci Rep 11, 11187. https://doi.org/10.1038/s41598-021-90541-8.
Dungworth, D., 2009. Kelp in historic glass: the application of strontium isotope analysis (Dungworth, Degryse and Schneider). Isotopes in Vitreous Materials.
Foster, H.E., Jackson, C.M., 2009. The composition of 'naturally coloured' late Roman vessel glass from Britain and the implications for models of glass production and supply. J. Archaeol. Sci. 36, 189–204. https://doi.org/10.1016/J.JAS.2008.08.008.
Foster, H.E., Jackson, C.M., 2010. The composition of late Romano-British colourless vessel glass: glass production and consumption. J. Archaeol. Sci. 37, 3068–3080. https://doi.org/10.1016/J.JAS.2010.07.007.
Foy, D., Nenna, M.-D., 2001. Tout feu tout sable: mille ans de verre antique dans le Midi de la France : [exposition], musée d'histoire de Marseille, [2001]. Edisud; Musées de Marseille, Aix-en-Povence, Marseille.
Foy, D., Picon, M., Vichy, M., Thirion-Merle, V., 2003. Characterization of glasses from the end of Antiquity in the Western Mediterranean: the emergence of new commercial currents, in: Exchanges and trade in glass in the ancient world. Presented at the international colloquium of AFAV, Aix-en -Provence and Marseille, June 2001, Monographs Instrumentum 24, Montagnac, pp. 41–86.
Freestone, I.C., 2005. The Provenance of Ancient Glass through Compositional Analysis. MRS Proc. 852 (OO8), 1. https://doi.org/10.1557/PROC-852-OO8.1.
Freestone, I.C., Gorin-Rosen, Y., Hughes, M.J., 2000. Primary glass from Israel and the production of glass in late antiquity and the early Islamic period. Travaux de la Maison de l'Orient 65–88.
Freestone, I.C., Ponting, M., Hughes, M.J., 2002. The origins of Byzantine glass from Maroni Petrera, Cyprus. Archaeometry 44, 257–272. https://doi.org/10.1111/1475-4754.T01-1-00058.
Freestone, I.C., Leslie, K.A., Thirlwall, M., Gorin-Rosen, Y., 2003. Strontium Isotopes in the Investigation of Early Glass Production: Byzantine and Early Islamic Glass from the Near East*. Archaeometry 45, 19–32. https://doi.org/10.1111/1475-4754.00094.
Freestone, I., 2003. Primary glass sources in the mid-first millennium A.D. Freestone I C (2003) Primary glass sources in the mid-first millennium A.D. Annales du 15e Congres de l'Association Internationale pour l'Histoire du Verre, 111-115.
Freestone, I.C., 2015. The Recycling and Reuse of Roman Glass: Analytical Approaches 13.
Gallo, F., Silvestri, A., Molin, G., 2013. Glass from the Archaeological Museum of Adria (North-East Italy): new insights into Early Roman production technologies. J. Archaeol. Sci. 40, 2589–2605. https://doi.org/10.1016/j.jas.2013.01.017.
Gliozzo, E., 2017. The composition of colourless glass: a review. Archaeol. Anthropol. Sci. 9, 455–483. https://doi.org/10.1007/S12520-016-0388-Y/TABLES/9.
Gratuze, B., Giovagnoli, A., Barrandon, J.N., Telouk, P., Imbert, J.L., 1993. Apport de la méthode ICP-MS couplée à l'ablation laser pour la caractérisation des archéomatériaux. Revue d'Archéométrie 17, 89–104.
Gratuze, B., Blet-Lemarquand, M., Barrandon, J.-N., 2001. Mass spectrometry with laser sampling: A new tool to characterize archaeological materials. J. Radioanal. Nucl. Chem. 247, 645–656.
Gratuze B., 2013. Glass Characterisation Using Laser Ablation Inductively Coupled Plasma Mass Spectrometry Methods, In book: Modern Methods for Analysing Archaeological and Historical Glass (pp.201-234), DOI: 10.1002/9781118314234.ch9.
Groh, S., 2011. Ricerche sull'urbanistica e le fortificazioni tardoartiche e bizantine di Aquileia. Relazioni sulle prospezioni geofisiche condotte nel 2011. Aquileia Nostra 82, 153–204.
Henderson, J., 1985. The raw materials of early glass production. Oxf. J. Archaeol. 4, 267–291. https://doi.org/10.1111/J.1468-0092.1985.TB00248.X.
Jaćimović, R., Smodiš, B., Bučar, T., Stegnar, P., 2003. k0-NAA quality assessment by analysis of different certified reference materials using the KAYZERO/SOLCOI software. Journal of Radioanalytical and Nuclear Chemistry 2003 257:3 257, 659–663. 10.1023/A:1026116916580.
Jackson, C.M., 2005. Making colourless glass in the Roman period. Archaeometry 47, 763–780. https://doi.org/10.1111/j.1475-4754.2005.00231.x.
Jackson, C., Cottam, S., 2015a. The green, green glass of Rome. Presented at the Annales du 19e Congres de l'AIHV 2012, pp. 109–117.
Jackson, C.M., Cottam, S., 2015b. "A green thought in a green shade"; Compositional and typological observations concerning the production of emerald green glass vessels in the 1st century A.D. J. Archaeol. Sci. 61, 139–148. https://doi.org/10.1016/J.JAS.2015.05.004.
Jackson, C.M., Paynter, S., 2016. A Great Big Melting Pot: Exploring Patterns of Glass Supply, Consumption and Recycling in Roman Coppergate, York. Archaeometry 58, 68–95. https://doi.org/10.1111/arcm.12158.
Jackson, C.M., Paynter, S., Nenna, M.D., Degryse, P., 2018. Glassmaking using natron from el-Barnugi (Egypt); Pliny and the Roman glass industry. Archaeol. Anthropol. Sci. 10, 1179–1191. https://doi.org/10.1007/S12520-016-0447-4/FIGURES/6.
Lankton J., Pulak C., Gratuze B., (2022b). Glass ingots from the Uluburun shipwreck: Addition of glass cullet during manufacture and evidence for the changing context of New Kingdom Egyptian glass production in the late 18th Dynasty, Journal of Archaeological Science: Reports 45(4):103596 (2022), DOI: 10.1016/j.jasrep.2022.103596.
Lankton, J., Pulak, C., Gratuze, B., 2022a. Glass ingots from the Uluburun shipwreck: Glass by the batch in the Late Bronze Age. J. Archaeol. Sci. Rep. 42 (3), 103354 https://doi.org/10.1016/j.jasrep.2022.103354.
Lepri, B., Saguì, L., 2018. Vetri e indicatori di produzione vetraria a Ostia e a Porto. Mélanges de l'École française de Rome - Antiquité 399–409 https://doi.org/10.4000/mefra.6506.
Maltoni, S., Silvestri, A., Marcante, A., Molin, G., 2016. The transition from Roman to Late Antique glass: new insights from the Domus of Tito Macro in Aquileia (Italy). J. Archaeol. Sci. 73, 1–16. https://doi.org/10.1016/J.JAS.2016.07.002.
Mirti, P., Lepora, A., Saguì, L., 2000. Scientific analysis of seventh-century glass fragments from the crypta Balbi in Rome*. Archaeometry 42, 359–374. https://doi.org/10.1111/J.1475-4754.2000.TB00887.X.
Mirti, P., Davit, P., Gulmini, M., Sagui, L., 2001. Glass Fragments from the Crypta Balbi in Rome: the Composition of Eighth-Century Fragments. Archaeometry 43 (4), 491–502.
Mirti, P., Pace, M., Negro Ponzi, M.M., Aceto, M., 2008. ICP–MS analysis of glass fragments of Parthian and Sasanian epoch from Seleucia and Veh Ardašīr (central Iraq). Archaeometry 50, 429–450. https://doi.org/10.1111/j.1475-4754.2007.00344.x.
Nenna, M.-D., Vichy, M., Picon, M., 1997. L'atelier de verrier de Lyon, du Ier siècle apr. J.-C., et l'origine des verres « romains ». ArchéoSciences, revue d'Archéométrie 21, 81–87. https://doi.org/10.3406/ARSCI.1997.949.
Nikita, K., Nightingale, G., 2006. An archaeological and scientific study of Mycenaean glass from Elateia-Alonaki, Greece, in: Annals of the 17th Congress of the International Association for the History of Glass. Antwerp, pp. 39–46.
Panighello, S., Van Elteren, J.T., Orsega, E.F., Moretto, L.M., 2015. Laser ablation-ICP-MS depth profiling to study ancient glass surface degradation. Anal. Bioanal. Chem. 407, 3377–3391. https://doi.org/10.1007/s00216-015-8568-7.
Paynter, S., Jackson, C.M., 2018. Mellow yellow: An experiment in amber. J. Archaeol. Sci. Rep. 22, 568–576. https://doi.org/10.1016/J.JASREP.2017.11.038.
Paynter, S., Jackson, C., 2019. Clarity and brilliance: antimony in colourless natron glass explored using Roman glass found in Britain. Archaeol Anthropol Sci 11, 1533–1551. https://doi.org/10.1007/s12520-017-0591-5.
Price, J., 2005. Glass-working and glassworkers in cities and towns. In: MacMahon, A., Price, J. (Eds.), Roman working lives and urban living. Oxbow, Oxford, pp. 167–190.
Price, J., Cottam, S., 1998. Romano-British Glass Vessels: A Handbook. CBA, Walmgate, York.
Rehren, T., Freestone, I.C., 2015. Ancient glass: From kaleidoscope to crystal ball. J. Archaeol. Sci. 56, 233–241. https://doi.org/10.1016/j.jas.2015.02.021.
Sanderson, D., Hutchings, J., 1987. The origins and measurement of colour in archaeological glasses. Glass Technol.
Sayre, E.V., 1963. The intentional use of antimony and manganese in ancient glasses. In: Matson, F.R., Rindone, G.E. (Eds.), VI International Congress on Glass: Advances in glass technology: history papers and discussions of the technical papers. Plenum Press, New York, pp. 263–282.
Sayre, E.V., 1964. Some ancient glass specimens with compositions of particular archaeological significance. Brookhaven National Laboratory report BNL 879 T-354, Chemistry-TID-4500, New York.
Schibille, N., Sterrett-Krause, A., Freestone, I.C., 2017. Glass groups, glass supply and recycling in late Roman Carthage. Archaeol. Anthropol. Sci. 9, 1223–1241. https://doi.org/10.1007/s12520-016-0316-1.
Schibille, N., Patrice, L., Biron, I., Brunswic, L., Blondeau, E., Gratuze, B., 2022. Origins and manufacture of the glass mosaic tesserae from the great Umayyad Mosque in Damascus. J. Archaeol. Sci. 147, 105675 https://doi.org/10.1016/j.jas.2022.105675.
Schreurs, J.W.H., Brill, R.H., 1984. Iron and sulfur related colors in ancient glasses. Archaeometry 26, 199–209. https://doi.org/10.1111/J.1475-4754.1984.TB00334.X.
Shepherd, J.D., 2009. The glass workers of Roman London / John Shepherd and Angela Wardle; with Mark Taylor and David Hill; photography by Andy Chopping. Museum of London Archaeology, London.
Silvestri, A., 2008. The coloured glass of Iulia Felix. J. Archaeol. Sci. 35, 1489–1501. https://doi.org/10.1016/j.jas.2007.10.014.
Silvestri, A., Gallo, F., Maltoni, S., Degryse, P., Ganio, M., Longinelli, A., Molin, G., 2018. Things that travelled - A review of the Roman glass from Northern Adriatic Italy, in: Things That Travelled - Mediterranean Glass in the First Millennium AD.
Silvestri, A., Molin, G., Salviulo, G., 2008. The colourless glass of Iulia Felix. J. Archaeol. Sci. 35, 331–341. https://doi.org/10.1016/j.jas.2007.03.010.
Stern, E.M., 2002. Glass Is Hot. Am. J. Archaeol. 106, 463–471. https://doi.org/10.2307/4126284.
Traviglia, A., Panighello, S., Moretto, L., Orsega, E.F., Bernardoni, A., Floreani, S., Moro, G., Mandruzzato, L., 2021. Picking up the hint: raw glass chunks and glass wastes from ploughsoil collection in Aquileia (Italy), in: G. Balint, Antala, B., Carty, C., Mabieme, J.-M.A., Amar, I.B., Kaplanova, A. (Eds.), Uniwersytet Śląski. İstanbul, pp. 255–264. 10.2/JQUERY.MIN.JS.
Van Der Linden, V., Cosyns, P., Schalm, O., Cagno, S., Nys, K., Janssens, K., Nowak, A., Wagner, B., Bulska, E., 2009. Deeply coloured and black glass in the northern provinces of the Roman empire: Differences and similarities in chemical composition before and after AD 150. Archaeometry 51, 822–844. https://doi.org/10.1111/j.1475-4754.2008.00434.x.
Van Elteren, J.T., Tennent, N.H., Šelih, V.S., 2009. Multi-element quantification of ancient/historic glasses by laser ablation inductively coupled plasma mass spectrometry using sum normalization calibration. Anal. Chim. Acta 644, 1–9. https://doi.org/10.1016/J.ACA.2009.04.025.
Velde, B., 1990. Alumina and calcium oxide content of glass found in western and northern Europe, first to ninth centuries. Oxford J. Archaeol. 9, 105–117.

Vicenzi, E.P., Eggins, S., Logan, A., Wysoczanski, R., 2002. Microbeam Characterization of Corning Archeological Reference Glasses: New Additions to the Smithsonian Microbeam Standard Collection. undefined 107, 719–727. 10.6028/JRES.107.058.

Wagner, B., Nowak, A., Bulska, E., Kunicki-Goldfinger, J., Schalm, O., Janssens, K., 2008. Complementary analysis of historical glass by scanning electron microscopy with energy dispersive X-ray spectroscopy and laser ablation inductively coupled plasma mass spectrometry. Microchim Acta 162, 415–424. https://doi.org/10.1007/s00604-007-0835-7.

Wagner, B., Nowak, A., Bulska, E., Hametner, K., Günther, D., 2012. Critical assessment of the elemental composition of Corning archeological reference glasses by LA-ICP-MS. Anal. Bioanal. Chem. 402, 1667–1677. https://doi.org/10.1007/s00216-011-5597-8.

Wedepohl, K.H., Baumann, A., 2000. The Use of Marine Molluskan Shells for Roman Glass and Local Raw Glass Production in the Eifel Area (Western Germany). Naturwissenschaften 2000 87:3 87, 129–132. 10.1007/S001140050690.

Wedepohl, K.H., Simon, K., Kronz, A., 2011. Data on 61 chemical elements for the characterization of three major glass compositions in Late Antiquity and the Middle Ages. Archaeometry 53, 81–102.

World, G.-R., 2014. Glass Making in the Greco-Roman World: Results of the ARCHGLASS project. Glass Making in the Greco-Roman World: Results of the ARCHGLASS project 190. 10.26530/OAPEN_513796.